Meas. Sci. Technol. 5 (1994) 1389–1395. Printed in the UK

A 60 Joule, 600 kV, 500 ps risetime, 60 ns pulse width Marx generator

M M Kekez and J Liu

National Research Council of Canada, Ottawa, Canada K1A OR6

Received 19 July 1994, in final form 2 September 1994, accepted for publication 13 September 1994

Abstract. The experimental and computer modelling of the performance of a 24-stage coaxial line Marx generator are presented. Internal inductance, stray capacitance, coupling capacitance between the stages and switch characteristic are considered. The detailed geometry of each stage and of the total system is included in the computer simulation. The uv pre-ionized spark gaps forming the switches in the system are characterized by the spark overvoltage. The transmission line effects are also observed. The output characteristics are given at different overvoltages. With a peaking circuit placed at the output of the Marx generator, the risetime of the output pulse was enhanced from 2–4 ns to 0.4–0.6 ns at the 600 kV level.

1. Introduction

Because of their simplicity, reliability and versatility, Marx generators have been used for a number of years as a prime driver to facilitate (a) intense relativistic electron/ion beams needed for high-power microwave generation, (b) a source for flash x-ray radiography to record dynamic events where interposed material, debris or flames exclude the use of high speed cameras, (c) electromagnetic pulse (EMP), (d) a generator for dielectric study, (e) pre-ionization for the excimer lasers, and so on.

Hewlett-Packard Ltd has been manufacturing such a flash x-ray/electron beam system for a long time, while the Physics International Company and Maxwell Laboratories Inc. provide sophisticated set-ups to meet specific demands for a number of fields. Novel concepts to speed up the risetime at low voltage (circa 1–2 kV) pulses have been recently proposed by Baker *et al* (1993) and Bolton *et al* (1994).

The discussion in this paper is limited to the design of medium (tens to several kilojoules) sized, moderately high voltage (600 or 1000 kV and scalable to 4 MV) systems, leading to a fast pulse (coaxial) line that readily competes with commercial systems in terms of both cost and performance.

In an earlier paper by Kekez *et al* (1989), preliminary experimental results together with some computer simulations were presented. Further work by Kekez (1991) led to the development of an ultra-fast compact Marx system and the concept of precisely timed switches was introduced.

With the advent of powerful circuit software, e.g. PSpice, it is possible to analyse the system in great detail and to improve the overall features of the generator. In particular, it is important to appreciate the proposed sequential erection of the system at precise time intervals and to relate these time intervals to the degree of switch overvoltage.

It is also necessary to understand why the reproducibility of the experimental results is so good, since the breakdown process has a statistical component. The deviations were simulated in the Marx to find whether there is a self-imposed correction in sequentially fired switches with respect to the overvoltage and/or timing.

2. Formulation

The Marx generator (figure 1 (top)) can be viewed as a distributed transmission-storage line, consisting of 24 cascaded stages. Each stage has three 2.7 nF, 40 kV Murata capacitors connected in parallel for an energy storage capacitance C. The metallic enclosure forms a transmission line with characteristic impedance, Z_0, with a time transit time, T_D. For each stage, a UV pre-ionized spark gap switch S with associated series inductance, L, and stray capacitance of the spark gap electrode with respect to the ground, C_s, were also considered. The parasitic coupling capacitance, C_c, formed between the facing plates of the energy storage capacitance is also included.

The Marx is modelled using lumped and distributed parameters figure 1 (bottom). The position of each of the Marx components with respect to the enclosure is found to be equivalent to one of a lumped inductance,

0957-0233/94/111389+07$19.50

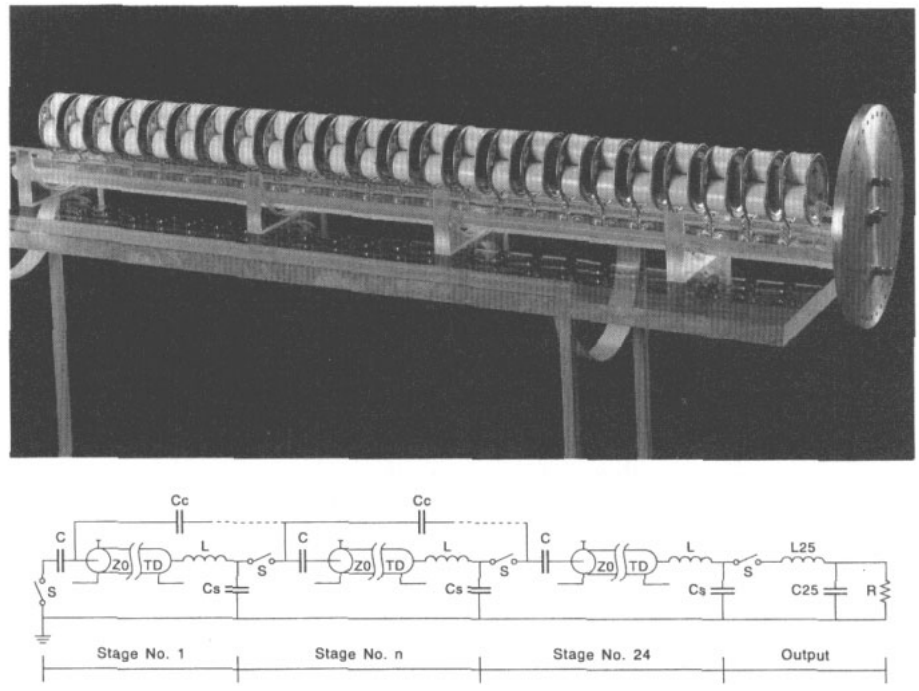

Figure 1. Top: stage assembly of a 24-stage Marx generator. Bottom: schematic diagram.

capacitance or short transmission line. Since the simulated output waveform is a strong function of the switch firing sequence, detailed studies were carried out. The computer simulations allowed the experimental timing data to deviate by ±10%.

It was suggested by Kekez (1991) that, when the first stage is activated, the stray capacitance C_s permits the current flow in the first stage even if the second switch is permanently open (see figure 1 (bottom)). When the transmission line is neglected, this allows a smooth oscillating current waveform. Since $C \gg C_s$, the voltage at C is transferred at C_s making the voltage across the switch in the second stage 2 V. If, at this time of a 1/4 period, breakdown occurs, the second switch will experience 100% of overvoltage. This analysis considers that all the stages in the Marx will be erected in a sequential manner at precise time intervals.

With the introduction of a transmission line effect, it is expected that the voltage will double, since the line is an open circuit, e.g. the next switch in sequence is not yet closed.

Let us now ask: what is the degree of overvoltage in the real system? The experimental data and the simulation will be compared.

3. Estimation of circuit parameters in a stage

3.1. Inductance

The total inductance consists of the lumped parts: a capacitor inductance L_c, a spark gap channel inductance L_g, and the connection of the leads between spark gap and the capacitor L_l. Due to the finite dimension of the capacitor, the transmission line inductance L_t, is included.

The leads of the capacitors with respect to the enclosure can be approximated by off-centred coaxial structures. The self-inductance for each lead is 2.12 nH. Using the expression given by Lewis and Wells (1954), mutual inductances of 11.44, 12.12 and 12.12 nH are derived for each of the three condensers included in the assembly. The total value of L_c ($1/L_c = 1/(11.44 + 2.12) + 1/(12.12 + 2.12) + 1/(12.12 + 2.12)$ is 4.7 nH.

The transmission line (to represent three parallel Murata capacitors sandwiched in two metal plates) is also approximated by an off-centred coaxial line with $L_t = 13.50$ nH and the inductance of a spark gap channel L_g is taken to be 10 nH. (For information on L_g see J C Martin 1965, T H Martin 1989 amongst others). A lower limit of overall inductance ($L_c + L_g + L_t$) is estimated to be 28.20 nH.

3.2. Capacitance

The stray capacitance, C_{ss} consists of two 1 inch spheres and the transmission line capacitance, C_{st}. The expression of Kuffel and Zaengl (1984) was used to calculate C_{ss}. For our dimensions the capacitance of sphere–sphere is 1.81 pF and the capacitance of sphere–ground is 1.68 pF. As a result, the total value of C_{ss} is $1.68 + (1.68 \times 1.81)/(1.68 + 1.81) = 2.55$ pF.

The capacitance for an off-centred coaxial transmission line, C_{st} is 5.71 pF. Hence, total stray capacitance C_s is 8.26 pF.

The parasitic coupling capacitance C_c comes from

the metal plates that hold the (energy storage) capacitors; it is 4 pF.

3.3. Characteristic impedance

The characteristic impedance is $Z_0 = (L_t/C_{st})^{1/2}$. For our dimensions $Z_0 = 48.6\ \Omega$. Because of the complexity of the real structure, this calculation is tentative. The actual L_t could be larger than 13.50 nH, C_{st} smaller than 5.71 pF putting Z_0 in the range 48.6–100 Ω. The time delay of each stage T_D (= length/wave velocity) is 0.28 ns.

3.4. High voltage sensors

The following two types of sensor were employed:

(1) NRC developed wide-band (300 kHz to 3 GHz) capacitive E-field probe introduced by Fletcher (1949). Some features of the probe were determined using a network analyser and were compared to those of a monopole (E-dot) sensor. Our E-field probe has no resonant interactions. Excellent agreement between E-dot and E-field probes was observed in the risetime measurement. Because the calibration value may fluctuate over a six month period, these sensors were used only to measure the relative shapes of the waveform.

(2) Magnetic closed-loop probe (described by Seregelyi and Kashyap 1994) containing a model CT-1 current transformer (made by Tektronix Inc.) and a short circuited loop was used to measure the induced magnetic field. A part of this loop (1/4 inch) is exposed to the field and the remaining part is placed behind the ground plane. Because of its stable characteristics, it is employed for absolute measurement.

The probes were calibrated using the 'square' wave generator of the type described by Lewis and Wells (1954). The coaxial line of this generator is the same one used for the termination of the Marx generator. In this way the position of the probes remains fixed. More than two digit accuracy was achieved in the calibration of the probes.

4. Results and discussion

The experimental measurement of the output voltage (its shape, risetime, width and ringing frequency) is compared with simulations.

The measured waveform shown in figure 2(d) is obtained under conditions of 38 kV in SF_6 at 26 psi. It has a ringing frequency f_r of 142.9 MHz, risetime t_r of 3.35 ns and pulse width T_{pw} of 56 ns.

In the initial simulation by PSpice, it was assumed that $L = 28.20$ nH, $C_s = 8.26$ pF, the time interval between two adjacent switches is about 0.98 ns and the conductive resistance of the switch is 0.5 Ω. Also, a series inductance of 20 nH and a shunt capacitance of

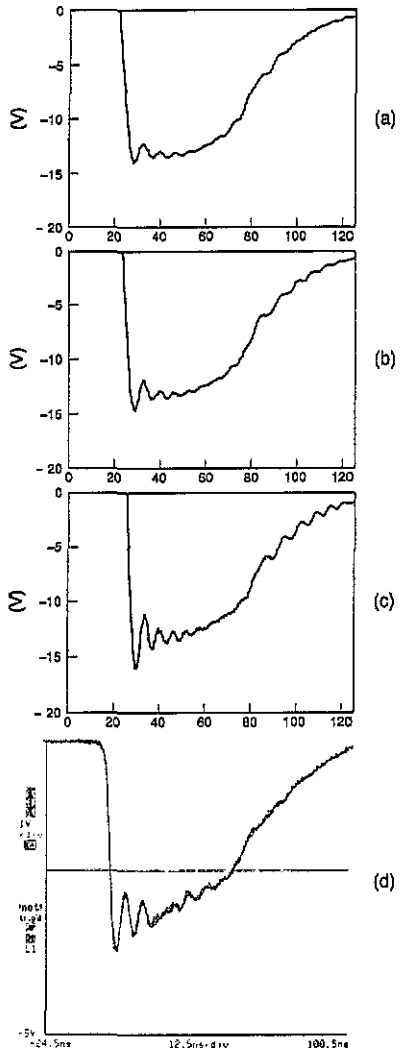

Figure 2. PSpice simulated waveform with $C = 8.4$ nF, $L = 65$ nH, $C_s = 8.5$ pF, $C_c = 4$ pF, $Z_0 = 100\ \Omega$, $T_D = 0.28$ ns, $R_{switch} = 0.5\ \Omega$, $R_{load} = 100\ \Omega$, $L_{25} = 20$ nH, $C_{25} = 4$ pF and for overvoltages of (a) 60%, (b) 110% and (c) 200%. Scale: charging voltage is 1 unit; 20 ns/div. Hence (zero-to-peak) efficiency with respect to charging voltage is: (a) 58%, (b) 61% and (c) 67%. (d) Five superimposed waveforms recorded with a 602 A digitizer, 0.5 GHz low-band filter and magnetic probe at 38 kV charging voltage per stage using SF_6 at 26 psi. Scale: 89 kV/div; 12.5 ns/div. Efficiency: 63%.

4 pF are included to represent L and C_s of the isolation switch placed at the output of the Marx bank.

With these parameters, the calculation shows that the width of the pulse is too small and that the ringing frequency is too high.

To get agreement with experiments, it is necessary to increase L from 28.20 nH to 65 nH and C_s from 8.26 pF to 8.5 pF. This yields $f_r = 138.9$ MHz, $t_r = 3.34$ ns and $T_{pw} = 55$ ns.

Without a transmission line and under the same conditions, one gets: $f_r = 190$ MHz, $t_r = 1.9$ ns and $T_{pw} = 40.7$ ns. Here, the width was found to be too short compared with the experimental results. Increasing inductance from 65 nH to 100 nH gives the following parameters: $f_r = 133.3$ MHz, $t_r = 3.3$ ns and $T_{pw} = 56$ ns, which agree well with the experimental findings. This implies that each section of transmission

line is equivalent to an additional inductance of 35 nH.

This observation can be appreciated by noting again the 'square' pulse generator by Lewis and Wells (1954). When their charged line is discharged into a matched load resistance, the duration of the square pulse is equal to twice the transit time of the charged transmission line.

Indeed, the results of this work confirm that the pulse stretched by $55-40.7 = 14.3$ ns, which is twice the total transit time of the transmission lines (2×24 stages $\times 0.28$ ns/stage).

In the work by Takagi *et al* (1979), Somerville (1989) and O'Malley and Buttram (1987), the transmission line effect was ignored. To get the correct parameters of the pulse, the authors must assume very large values of inductance, which in our opinion, could not be accounted for by only the geometrical considerations. For example, Somerville (1989) found that an extremely large inductance of 3.3 μH was needed to match the ringing frequency of 0.98 MHz in his Marx circuit. The contribution from capacitors L_c and spark gaps L_g to this 3.3 μH is only 300 nH. We disagree with his statement that the rest of the inductance of 3 μH is due to the single loop of the Marx circuit and the connections between the spark gap and the capacitor.

Figure 2 shows the waveforms at different values of overvoltage of 60% in (a), 110% in (b) and 200% in (c).

The condition of 60% overvoltage corresponds to sequential activation of the switches at precise equal time intervals of 0.90 ns. For higher overvoltage, the time interval for further stages decreases slightly. For 110% and 200% overvoltages, the average time intervals are 0.98 ns and 1.10 ns with decreasing rates in time intervals of 0.24% and 0.68% respectively. If the simulations are done under a constant time interval, the computed waveforms will have nearly identical features. This implies self-imposed correction in sequentially fired switches because, if the firing is delayed on any switch, the overvoltage would build up on the sequential switch and compensate for the delayed firing.

This conclusion is further supported by the following experimental evidence about the value of C_s which governs the timing sequence (analysis given by Kekez (1991)). For larger value of C_s, the waveform as in figure 2(a) was obtained. For smaller C_s, the waveform as in figure 2(c) was recorded. This was accomplished by changing the enclosure from solid tube to perforated one. Note that Z_0 only mildly affects the pulse width.

Figure 2 also shows that, as the overvoltage across the switch rises, the magnitude of the oscillatory waveform superimposed on the flat portion of the main impulse increases.

A rather square and smooth pulse is obtained if the coupling capacitance, C_c is neglected. With large C_c the pulse has a pronounced oscillation. The effect of C_c is similar to that of high overvoltage, as shown in figure 2(c) compared to figure 2(a).

Experimental values of the risetime of the Marx are given in figure 3.

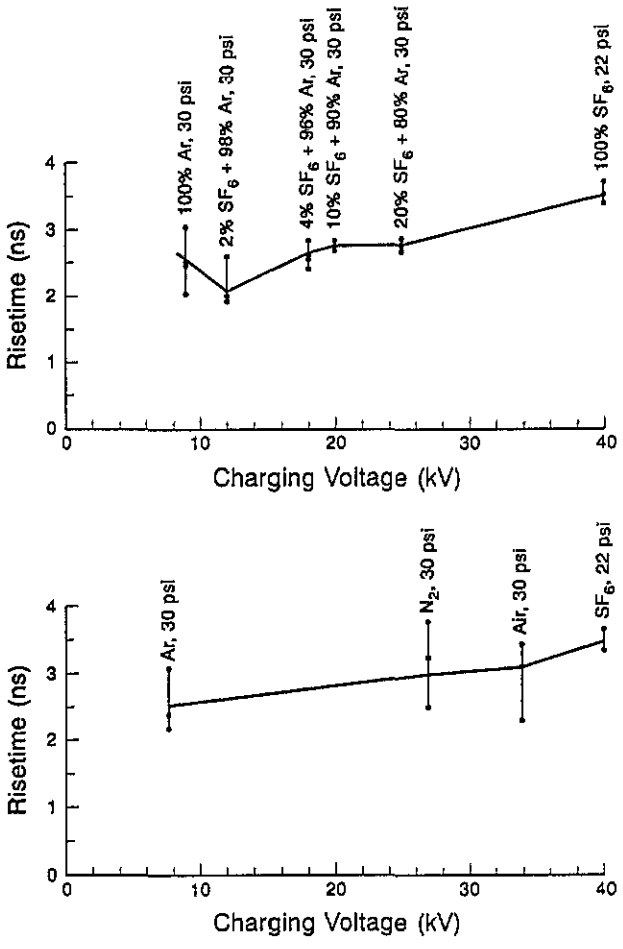

Figure 3. Risetime (measured internally by a 602 A digitizer, 0.5 GHz low-band filter and magnetic probe) as a function of the charging voltage for a gas mixture (top) and conventional gases (bottom).

5. Peaking circuit

A peaking circuit is designed to improve the risetime of the pulse generated by the Marx described above. It consists of an impedance transformer and a sliding spark gap (sharpening) switch (see figure 4(a)). The transformer matches the low output characteristic impedance of the Marx generator to that of the load (100 Ω). It is comprised of a short tapered coaxial line (the diameter of the inner cylinder decreases linearly from 14.6 cm to 5.72 cm with a length of 13.75 cm). The transformer is also designed to ensure that the height of the pre-pulse is nearly equal to that of the over-shoot.

In simulation, this transformer is approximated by 12 pieces of transmission line. The total capacitance used agrees with the measured capacitance of the assembly of 20 pF. If this capacitance is less than 10 pF, the overshoot is absent. For further discussion, see Harrison (1984).

The sharpening switch is a modified Maxwell spark gap, model 77073-1; a schematic diagram is shown in figure 4(b). All attempts were made to ensure that its geometry produces the minimum discontinuity in the central conductor. The copper ring was introduced to provide the seeds for ionization. This led to

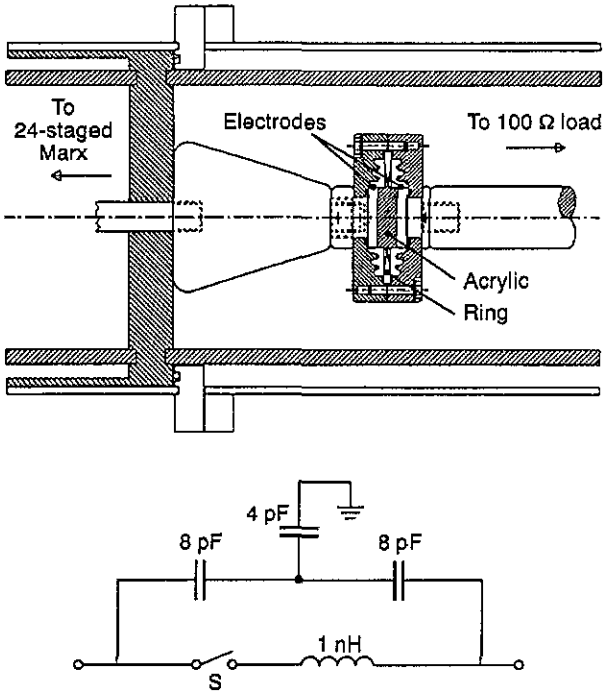

Figure 4. Experimental set-up of the peaking circuit (top) and schematic diagram of the sliding spark gap (bottom) with measured values of capacitances and estimated value of L. Here L enters via the L/R time constant. R = load = 100 Ω. The exact value of L is not critical.

establishment of multi-channelling (in the form of the current sheet) to slide along the acrylic insulator used.

The risetime can be controlled continuously by varying the pressure of the SF_6 and argon mixture in the switch. The experimental and computed results are shown in figure 5, where different diagnostics were used to acquire the same experimental data. Reproducibility of the experimental data is good.

The risetime measured as a function of pressure is shown in figure 6. Initially it decreases rapidly with increasing pressure, then slowly when it saturates at 0.4 ns. The calculated risetime and the curve have similar behaviour; however, the theoretical value saturates at about 0.26 ns.

6. Application

Marx generators are used for EMP study. A lot of effort is directed towards deriving the method for unifying electromagnetic standards and procedures and simplifying the design and testing of hardening techniques.

The following should demonstrate that the peak value of a threat required in the hardening procedures, occurs in a very short time, which demands very fast risetimes.

Let us assume that the pulse generated by a Marx bank drives the electronics components/systems via suitable antenna. The Joule energy density is

$$W = \int_0^\infty \sigma j^2 \mathrm{d}t \qquad (1)$$

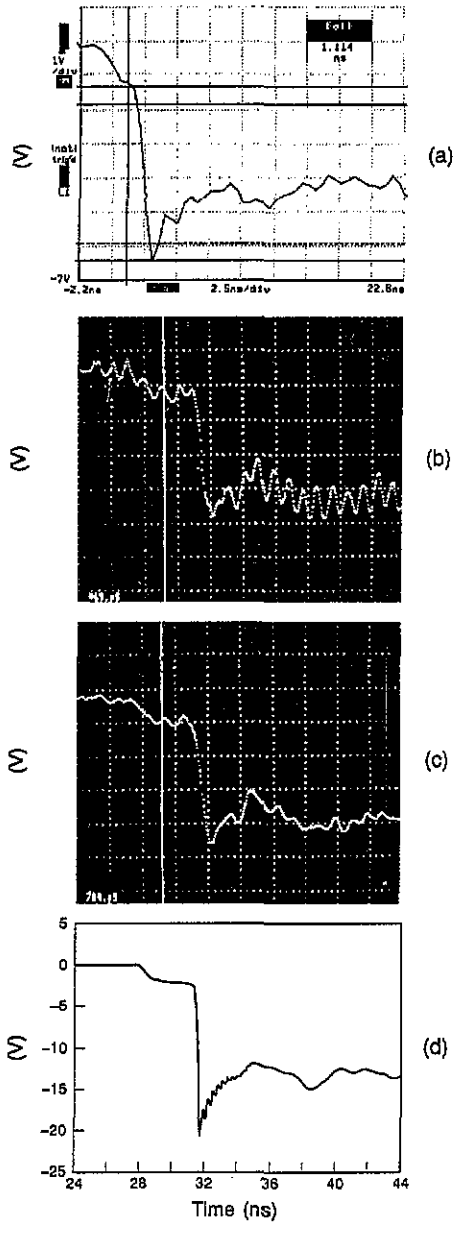

Figure 5. 'Rising' portion of waveforms. Peaking circuit is used. Other conditions as in figure 2(c). (a) After a pre-pulse indicated by vertical line a risetime t_r of 1.114 ns is recorded with a 602 A digitizer and a magnetic probe. Scale: 89 kV/div, 2.5 ns/div. (b) With a 7250 digitizer and a capacitive probe; t_r = 0.469 ns (see bottom left-hand corner). High (1.2 GHz) frequency oscillation is also present; its origin is not clear. (c) As (b) but with a 1 GHz low band filter; t_r = 0.704 ns. For (b) and (c) time scale: 2 ns/div. (d) Computation: t_r = 0.26 ns, and with 3 GHz low band filter, t_r = 0.49 ns. Scale 2 ns/div. (Zero to peak) efficiency: 85%.

where j is the displacement current density and is given by

$$j = \varepsilon \frac{\mathrm{d}E}{\mathrm{d}t}$$

where ε is the dielectric constant of the medium (air) and σ is the conductivity of the semiconductor device.

Instead of the time-domain presentation used in equation (1), it is customary to approach the task from the frequency domain. For further discussion, see Dion *et al* (1994).

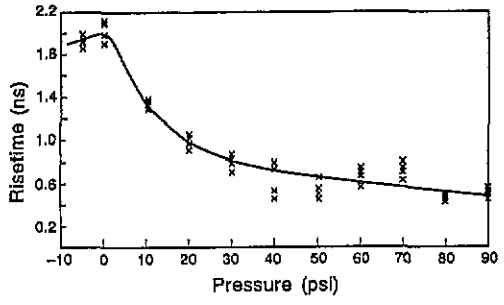

Figure 6. Risetime versus pressure in the sliding spark gap. A capacitive probe, 7250 digitizer and a 1 GHz low-band filter were used.

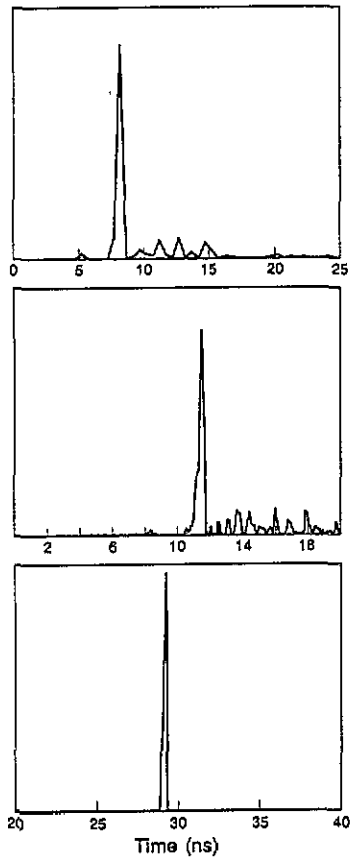

Figure 7. Displacement pulsed power (proportional to I^2) Recorded by a 602 A digitizer (top), a 7250 digitizer (middle) and computer simulation (bottom).

It has been argued that semiconductive components respond not only to the Joule energy, but also to the rate of change of the energy. Let us suppose that we have an EMP impulse with linear ramp from zero value to V_0 in a time interval, t_0. Here, t_0 would correspond to the risetime. If t_0 is decreased by a factor of n, then the power density will rise n^2 and the Joule energy will increase n times. For the data given in figure 5, the rate of change of the Joule energy is depicted in figure 7 as a narrow pulse of the duration equal to that of the risetime. Other features of the pulse are virtually irrelevant.

7. Conclusion

The present experimental results are well accounted for by a PSpice computer simulation. It was found that the finite sizes of the Marx components are equivalent to an additional inductance. This explains the phenomena that pulses of longer duration than expected are always obtained when small energy (20–100 Joule) high voltage (200–600 kV) generators are considered. Different combination of gases and gas mixtures gave excellent linearity in the output voltage for varying voltage per stage from about 8 to 40 kV. A peaking circuit offers a reliable method to improve the risetime from 2–4 ns to 0.5 ns.

Acknowledgments

The authors are indebted to Dr C Gardner for directing some parts of this work. We thank Dr S C Kashyap for his contributions. This project was partially supported by the Defence Research Establishment Ottawa. Interest shown by Dr F R S Clark and Mr J Arnold in this work is fully acknowledged. Thanks are also due to Messrs P R Cook and J G Dunn for their work on the experimental data acquisition. The technical drawings were prepared by Mr K Schoenherr, and the components were made in the workshops supervised by Mr S F Bouchard.

References

Baker R J, Hodder D J, Johnson B P, Subedi P C and Williams D C 1993 Generation of kilovolt-subnanosecond pulses using a nonlinear transmission line *Meas. Sci. Technol.* 4 893–5

Bolton H R, Dolan J E, Shapland A J, Parkes D M, Trafford K and Kerr B 1994 Investigations into 1 sub-ns pulse generation using ferrite-loaded coaxial lines *AGARD-DRG Symp., Ottawa, Canada, 2–5 May*

Dion M, Gardner C L and Kashyap S 1994 Hardening against a combined electromagnetic threat *AGARD-DRG Symp., Ottawa, Canada, 2–5 May*

Fletcher R C 1949 Production and measurement of ultra-high speed impulses *Rev. Sci. Instrum.* **20** 861–9

Harrison J L 1984 Circuit and electromagnetic system design notes *Note 41* Maxwell Laboratories Inc., 8888 Baboa Avenue, San Diego, CA 92123, USA

Hollmann B Z 1987 Net II simulation of a pulse forming line with spark gap and load *6th IEEE Pulsed Power Conf., Arlington, Virginia* pp 664–67

Kekez M M, LoVetri J, Podgorski A S, Dunn J G and Gibson G 1989 A 60 Joule, 600 kV, 1 ns rise-time Marx system *7th IEEE Pulsed Power Conference, Monterey, California* pp 123–7

Kekez M M 1991 Simple sub-50 ps rise time high voltage generator *Rev. Sci. Instrum.* **62** 2923–30

Kuffel E and Zaengl W S 1984 *High Voltage Engineering Fundamentals* (Oxford: Pergamon) pp 224–7

Lewis I A D and Wells F H 1954 Millimicrosecond Pulse Technique (Oxford: Pergamon) pp 100

Martin J C 1965 *AWRE Report No. SSWA/JCW/1065/25*

Martin T H 1989 An empirical formula for gas switch breakdown delay *7th IEEE Pulsed Power Conf., Monterey, California* pp 73–9

O'Malley M W and Buttram M T 1987 Development of a repetitive 1 MV, 22 kJ Marx generator *6th IEEE Pulsed Power Conf., Arlington, Virginia* pp 711–4

Seregelyi J S and Kashyap S 1994 Design, construction and calibration of HPM measurement *AGARD-DRG Symp., Ottawa, Canada, 2-5 May*

Smythe W R 1950 *Static and Dynamic Electricity* (New York: McGraw-Hill)

Somerville I C 1989 A simple compact 1 MV, 4 kJ Marx *7th IEEE Pulsed Power Conf., Monterey, California* pp 744–6

Takagi K, Kubota Y and Miyahara A 1979 Characteristics of co-axial Marx generator and its applicationto electron beam fusion *Japan. J. Appl. Phys.* **18** 1135–41

Taylor R S and Leopold K E 1984 UV radiation-triggered rail-gap switches *Rev. Sci. Instrum.* **55** 52–63